ISSN 2449-8955 European Journal of Biological Research *Research Article*

DOI: http://dx.doi.org/10.5281/zenodo.7487421

Impacts of prolonged exposure to low concentration of titanium dioxide nanoparticles on cell cycle control and DNA repair

Nada Elzahed, Andreas Kakarougkas *

Department of Biology, School of Sciences and Engineering, The American University in Cairo, Cairo 11835, Egypt

* Corresponding author e-mail: a.kakarougkas@aucegypt.edu

Received: 30 August 2022; **Revised submission:** 05 December 2022; **Accepted:** 27 December 2022

https://jbrodka.com/index.php/ejbr

ABSTRACT: Although the toxicological profile of titanium dioxide nanoparticles is not fully illuminated, large quantities of titanium dioxide nanoparticles (TiO_2NPs) are now produced. In our study, we evaluated the cytotoxic and genotoxic impacts of titanium dioxide nanoparticles on different cell lines (normal, cancer and DNA repair-deficient cells). MTT assay was used to evaluate the cytotoxicity, γ-H2AX and 53BP1 assay was used to evaluate the genotoxicity and G2/M assay was used to study the impacts of titanium dioxide nanoparticles on cell cycle regulation. In this study normal and DNA repair-deficient cell lines were used to study the repair mechanism of titanium dioxide nanoparticles induced DNA damage. G2/M checkpoint maintenance was also evaluated. We demonstrate that prolonged exposure to low concentrations of titanium dioxide nanoparticles does not induce significant cytotoxicity but induces significant genotoxicity, particularly DNA double-strand breaks (DNA DSBs). Furthermore, this study demonstrated that DNA DSBs at heterochromatin region are ATM-dependent and DNA DSBs at euchromatin region are ATM-independent and DNA PKcs dependent. After exposure to titanium dioxide nanoparticles, we show that the activation of G2/M checkpoint is DNA DSBs dependent threshold as does checkpoint release. All in all, we showed that prolonged exposure to low concentrations of titanium dioxide nanoparticles does not affect cell viability but causes DNA damage and cell cycle checkpoint adaptation which may lead to genetic instability.

Keywords: Medicinal plant; Antibacterial activity; Bacteria; Antioxidant activity; Free radical.

1. INTRODUCTION

1.1. Past Toxicological studies on TiO_2 NPs

One of the most widely produced nanomaterials are titanium dioxide nanoparticles (TiO_2 NPs), for its wide range of applications in everyday products. TiO_2 NPs increase the brightness of products, and resist decolorization [1]. Furthermore, titanium dioxide nanoparticles have a low price as raw material so it is commonly used in many products such as paints, food, cosmetics, and toothpastes [2]. Additionally, titanium dioxide nanoparticles have the ability to reflect UV-light and for that reason it is added in most sunscreens [3]. This clearly shows that titanium dioxide nanoparticles are widely used in essential products as a result millions of tons of titanium dioxide nanoparticles are produced every year.

The first to carry out toxicological profile of titanium dioxide in 1969 was the Joint FAO/WHO Expert Committee on food additives was the first to carry out toxicological evaluation of titanium dioxide in 1969 (JECFA1969), showing that titanium dioxide is insoluble and has no significant tissue absorption nor storage. Consequently, it was considered that titanium dioxide is biologically stable in human tissues [1] and does not cause lethality [4]. Subsequently, it was added by the Food and Drug Administration (FDA) in the United States as an Inactive Ingredient [1] and by the European Union (FAO/WHO 2010) as a primary food additive that is used in a wide range of consumer products. After the approval of the U.S. and EU for titanium dioxide to be added to the food additive list, and the huge range of applications that includes titanium dioxide nanoparticles, historical production of TiO_2 nanoparticles was observed making it one of the top 5 nanoparticles added in many products [5]. Eventually, concerns arose about the impact of titanium dioxides on human health. As a result, many *in vitro* and *in vivo* studies were carried out to evaluate titanium dioxide nanoparticles toxicity on human health. Such results will assist the governments with reliable data that can be used to re-evaluate the risk-benefit ratio of TiO_2 particles.

Most of the *in vitro* and *in vivo* studies were carried out to evaluate the toxicity of titanium dioxide nanoparticles on different cell lines. The International Agency for Research on Cancer and the National Institute for Occupational Safety and Health classified TiO_2 NPs as "possibly carcinogenic to humans" and as an" occupational carcinogen". This is because damage to major components of the cells such as protein, DNA and chromosomes was seen in many studies that showed immediately after exposure of cells to TiO_2 NPs[6]. Moreover, fragmentation of the nucleus, activation of caspase and cell death by apoptosis or necrosis was also reported [7].

In other studies, however, it was shown that cells can resist TiO_2 nanoparticle toxicity [8] which was further confirmed by many other studies, that the toxicity of TiO_2 is determined by the physicochemical properties of TiO_2 NPs and the type of cells that were included in the study. This indicates the importance of further studies in order to decipher the toxicity of TiO_2 NPs on different types of cells.

1.2. Limitations in the characterization DNA damage responses to TiO_2 NPs

As mentioned previously, TiO_2 NPs are one of the top 5 produced nanoparticles and have therefore been the subject of many toxicological studies. However, many of these studies have reported conflicting findings. It was reported by the International Program On Chemical Safety (1982) that most of the ingested titanium dioxide is not stored in the human body and is excreted in the urine. Additionally, some papers showed that TiO_2 NPs protect humans against UV-light-induced DNA damage and skin cancer [9]. Others show that TiO_2 NP can induce cell death in transformed cells [10]. However, other recent studies showed that TiO_2 NPs have the potential to induce genotoxicity and oxidative stress in important organs in mammals. These conflicting findings clearly show that there are unaddressed questions in this area that need to be further studied to ensure the safe use of titanium dioxide nanoparticles and to protect workers and consumers.

The main remaining gap in the studies carried out on evaluating the toxicity of TiO_2 NPs, is that the repair mechanisms for titanium dioxide-induced DNA damage are not fully highlighted as most of the studies focus on the DNA damage caused by the particles and not the repair mechanisms. Identifying the DNA repair pathways activated following NP exposure can help elucidate the cytotoxicity observed after exposure to TiO_2 NPs. This is because the presence of TiO_2 NPs in cells could also impair DNA Damage Responses (DDRs) as was previously observed in a study where exposure to TiO_2 NPs drastically impaired cellular DNA repair through both the NER and BER pathways [10]. One more study reported that cell death after exposure to

TiO_2NPs is due to the downregulation of DNA repair genes. These studies show that TiO_2 NPs can greatly impact the DDRs which can in turn impact genotoxicity and cytotoxicity. Therefore, further studies are needed to identify and explain the central steps involved in DNA repair mechanisms that are affected by exposure to TiO_2 NPs causing cellular death.

An additional limitation is that unrealistic scenarios are used in studies to test the toxicity of TiO_2 NPs on different cell lines. Cell lines were exposed to high concentrations of TiO_2 NPs, up to 200 micrograms per ml, for a short period of time [9]. These concentrations were shown to be 106-fold higher than human inhalation exposure in worst-case scenarios and more than the concentrations that individuals are exposed to during their whole life [11]. Thus, further studies using more practical scenarios are needed using low concentrations of the nanoparticles and for a longer period of time.

To fill the gaps, mechanisms that induce toxicity by NPs were tested in this study. We were able to achieve this by studying DNA damage, DNA repair and cell cycle control in normal, and DNA repair-deficient cell lines after exposure TiO_2 NPs. Importantly, more practical scenarios were used in this study by using prolonged exposure to very low concentrations of NPs. Finally, to investigate the therapeutic potential of TiO_2 NPs toxicity, the nanoparticles' toxicological profile was evaluated on normal vs. cancer cells.

2. MATERIALS AND METHODS

2.1. Chemicals and nanopowders

From Sigma Aldrich all chemicals and cell culture supplements were brought. Titanium (IV) oxide, nanopowder, 21nm primary particle size (TEM), >99.5% trace metal basis was obtained from sigma Aldrich (ref. 718467).

2.2. Nanoparticle dispersion

In fresh growth media, Dulbecco's Modified Eagle Medium, DMEM, powdered TiO_2 NPs were added, at a concentration of 200 μg/ml then NPs were sonicated for 30 mins using high power probe sonication (QSonica, Q700, Sonicator) in pulsed mode (1 s on/1 s off), at 4°C and 28% of amplitude before exposure to cells. The sonicated suspensions were diluted using growth media, DMEM, to give different concentrations from 0.1–200 μg/ml.

2.3. Cell culture

Seven cell lines were included in this study. These were:

1. 1 Br hTERT, immortalized normal human fibroblasts (Control)
2. WT, mouse embryo fibroblasts (Control)
3. U2OS, Human Bone Osteosarcoma epithelial cells,
4. A549, Adenocarcinoma human alveolar basal epithelial cells
5. ATM-/-, ATM mutated mouse embryo fibroblasts
6. ART-/-, Artemis defective mouse embryo fibroblasts
7. DNA Pkcs-/-, DNA-Pkcs defective mouse embryo fibroblasts

All cell lines were subcultured in fresh growth media, DMEM containing 4.5 g/1 glucose supplemented with 2 mM L-glutamine penicillin/streptomycin (50 IU/mL and 50 mg/ml, respectively) and 10% (vol/vol) fetal bovine serum (FBS). The cells were Kept at 37°C in a humidified 95% and 5% CO_2 air. The cells were passed when they reach confluency in T75 flask. The cells were obtained as a kind gift from the laboratory of Professor Penny Jeggo's laboratory (University of Sussex, UK).

2.4. MTT

Cytotoxicity was measured using the cell viability assay, the 3-[4,5-dimethylthiazol-2-yl]-2,5-diphenyl tetrazolium bromide (MTT) assay. Cells were allowed to grow to reach sub-confluency using 96-well plates before exposure to 100 µL of 0.1–200 µg/ml of NPs suspension for 24–168 hours. 100 µL of a 5 mg/ml MTT solution was added to each well after exposure to NPs. Cells were incubated for 4 hours at 370C in the dark, then the medium was removed and 100 µL of DMSO, dimethyl sulfoxide, was added and mixed for 1 minute on a plate reader's shaker until dissolving the formazan crystals. To eliminate the effect of the presence of residual NPs that could interfere with the absorbance, after dissolving the formazan crystals NPs were allowed to sediment and 50 µl from each well were transferred to another plate. Then, absorbance was measured at 570 nm wavelength and cell viability was then determined as a percentage of the negative control (unexposed cells).

2.5. Immunofluorescent staining using γ-H2AX and total 53BP1

Coverslips were used for the cells seeding in a 3 cm petri dish and then exposed to NPs. After exposure to NPs 3% formaldehyde was added to fix the cells for 10 minutes then cells were permeabilized by adding Triton X-100 in PBS for 3 mins. adding 100µl of anti-γ -H2AX and anti-53BP1 as primary antibodies (dilution 1/600, vol./vol in 2% BSA, bovine serum albumin) were then added for 1 hour at room temperature. Then PBS was used to wash the cells three times. Secondary antibodies 100 µl of FITC and TRITC (dilution 1/200, vol./vol. in 2% BSA, bovine serum albumin) were added for 1 hour at room temperature in a dark room. Cell nuclei were stained for 5 minutes with DAPI (0.005 mg/ml) in complete darkness. Coverslips were mounted on slides using fluorescein media for microscope analysis. Average numbers of green Foci that co-localized with red foci were measured per 50–100 cell nuclei, using an inverted microscope Olympus TM using WU and WB filters at wavelength ranges 358-461 and 495-570 nm respectively. Three slides were analyzed in each condition.

2.6. Phosphohistone H3 Immunofluorescent staining

12 wells plates were used for cell seeding overnight. NPs were added after cells reached the exponential phase. Then 3% formaldehyde was added for 10 minutes to fix the cells after NPs exposure. After fixation cells were washed with PBS and permeabilized with 0.1% Triton X-100 for 3 minutes and washed with PBS. Then the primary antibody for phosphorylated-H3 (100 µl) was added for 1 hour 1:300 in 2% BSA. This was followed by a secondary antibody 100µ l TRITC, for 1 hour 1:100 in 2% BSA in a dark room. DAPI was added for 5 minutes to stain cell nuclei (0.005mg/ml). Visualization was carried out using an inverted microscope Olympus TM using WU and WB filters at wavelength ranges 358-461 and 495-570 nm respectively. Three replicates were carried out and analyzed in each condition.

2.7. Statistics

All experiments were conducted in triplicate and the mean values were calculated. The significance of the difference in mean values between different conditions was assessed by the Student's T-test. The difference was considered significant when p-value is less than 0.05.

3. RESULTS

3.1. Cytotoxicity

Testing the survival and death rate after acute and prolonged exposure to the NPs provides insight into the short and long-term effect of the NP's cytotoxicity. Using the MTT assay, the cytotoxicity of TiO2 NPs was assessed in Human Bone osteosarcoma Epithelial cells (U2OS) (Fig. 1). After exposing the cells to different

concentrations of TiO_2 NPs from 0.1 to 200 μg/ml for different exposure times 24 and 168 hours, the percentage of cell viability was significantly reduced from 100% to 53% after 24 hours at the highest concentration used. However, no significant reduction in the percentage of cell viability was observed after 168 hours (Fig. 1). Although there was no cytotoxicity observed after 168 hours we hypothesized that genotoxicity was possibly induced and stabilized by the prolonged exposure TiO_2 NPs leading to cellular adaptation rather than cell death.

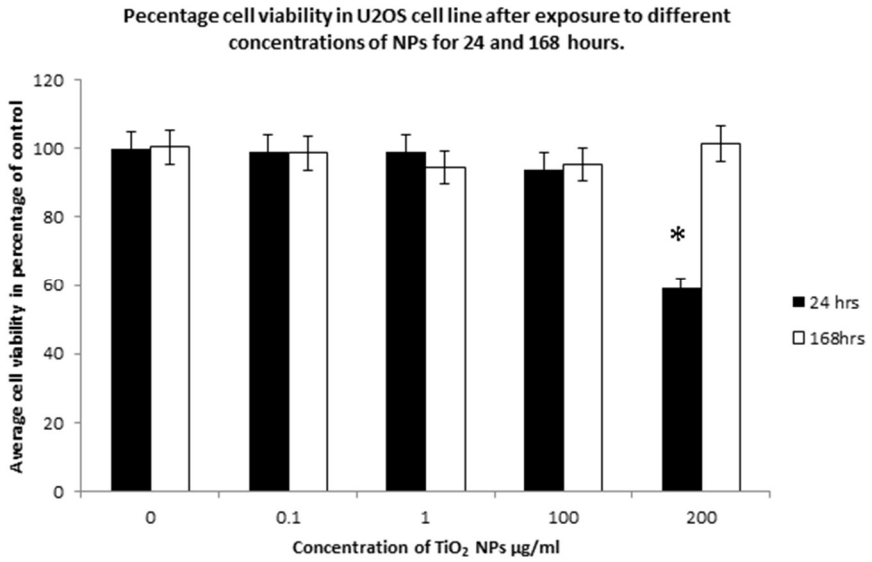

Figure 1. Evaluation of cytotoxicity induced by TiO_2 NPs in U2OS cell line. A significant concentration-dependent increase in cytotoxicity in U2OS cells was exposed for 24 hours ($P<0.05$). However, no significant cytotoxicity was observed after 168 hours ($P=0.2$). The data are expressed as mean values from three independent experiments, with n=6 in each independent experiment.

3.2. Genotoxicity

3.2.1. Immunofluorescent detection of DNA double-strand breaks (DNA DSBs) in U2OS, A549 and 1Br hTERT cell lines

Cytotoxicity is not the only biological marker that could reflect the toxicity of the NPs. This is because the NPs may induce genotoxicity without affecting cell survival leading to genomic instability rather than cell death. Therefore, we decided to evaluate the DNA damage induced by the NPs and to compare the amount of DNA damage induced over acute and prolonged exposure times. Different concentrations of TiONPs (0, 0.1, 0.5, 100, 200 μg/ml) were added to sub-confluent U2OS, A549 and 1Br hTERT cells for 24 and 168 hours. This was followed by fixation and immunofluorescent staining for γ-H2AX and 53BP1 (Fig. 2c). statistically Significant genotoxicity in a dose-dependent manner was obtained for the three cell lines. but no time-dependent genotoxicity was gained. As a result, on repeated exposure DNA repair may have arisen preventing the accumulation of DNA damage over 168 hours leading to no time-dependent genotoxicity (Fig. 2c).

3.2.2. Immunofluorescent visualization of double-strand breaks in WT, $ATM^{-/-}$, and DNA $PKcs^{-/-}$ cell lines

In order to visualize the lesions of DNA breaks induced by TiO_2 NPs and to identify which DNA repair kinetics pathway will be activated for repairing the DNA lesions, we synchronized WT, $ATM^{-/-}$ and DNA $PKcs^{-/-}$ mouse embryonic fibroblasts (MEFs) in G1 phase, cells were left to gain 100% confluency before treatment [12]. Then the three cell lines were exposed to 0.1 μg/ml TiO_2 for 24 hours (Fig. 3b).

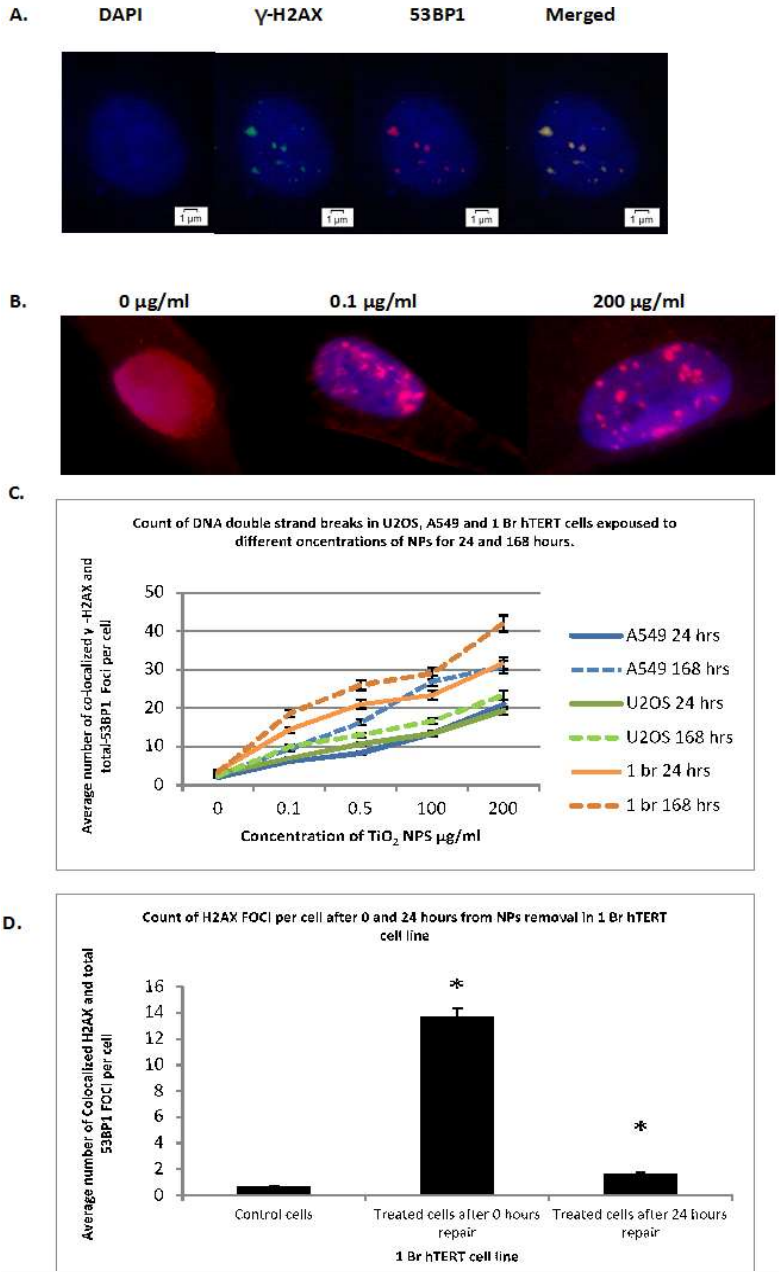

Figure 2. Immunofluorescent visualization and quantification of double-strand breaks in DNA using 1 Br hTERT, A549 and U2OS cell lines. (a) 2-D images showing DAPI staining for A549 cell nuclei (blue nuclei), staining of phosphorylated H2AX (γH2AX) (green foci) and total-53BP1 (red foci). 53BP1 were induced by TiO_2 NPs forming distinct foci which co-localized with γH2AX forming orange coloration foci in DAPI stained nucleus (b) 2-D images of 1 Br hTERT cells showing dose-dependent 53BP1 foci formation after exposure to different concentrations of TiO_2 NPs. (c) graph representing significant dose dependent curves for 1Br hTERT, U2OS and A549 cell lines ($p<0.05$) . The graph also shows insignificant time-dependent response curves in the three cell lines. Quantification of DNA double-strand breaks was performed by counting the mean number of co-localized γ-H2AX and total-53BP1 foci per cell in three different cell lines, 1 Br hTERT, U2OS and A549 after exposure to different concentrations of TiO_2 NPs (0-200 µg/ml) for 24 and 168 hours. Data shown are mean values calculated from three independent experiments. (d) the graph shows the mean number of co-localized γ-H2AX and total 53BP1 in 1Br hTERT cell after exposure to 0.1 µg/ml TiO_2 NPs for 24 hours then cells were allowed to repair for 0 and 24 hours after removal of nanoparticles results show a significant decline in the number of co-localized γ-H2AX and total 53BP1 foci between 0 and 24 hours repair ($P<0.05$). Represented data are mean values from three independent experiments.

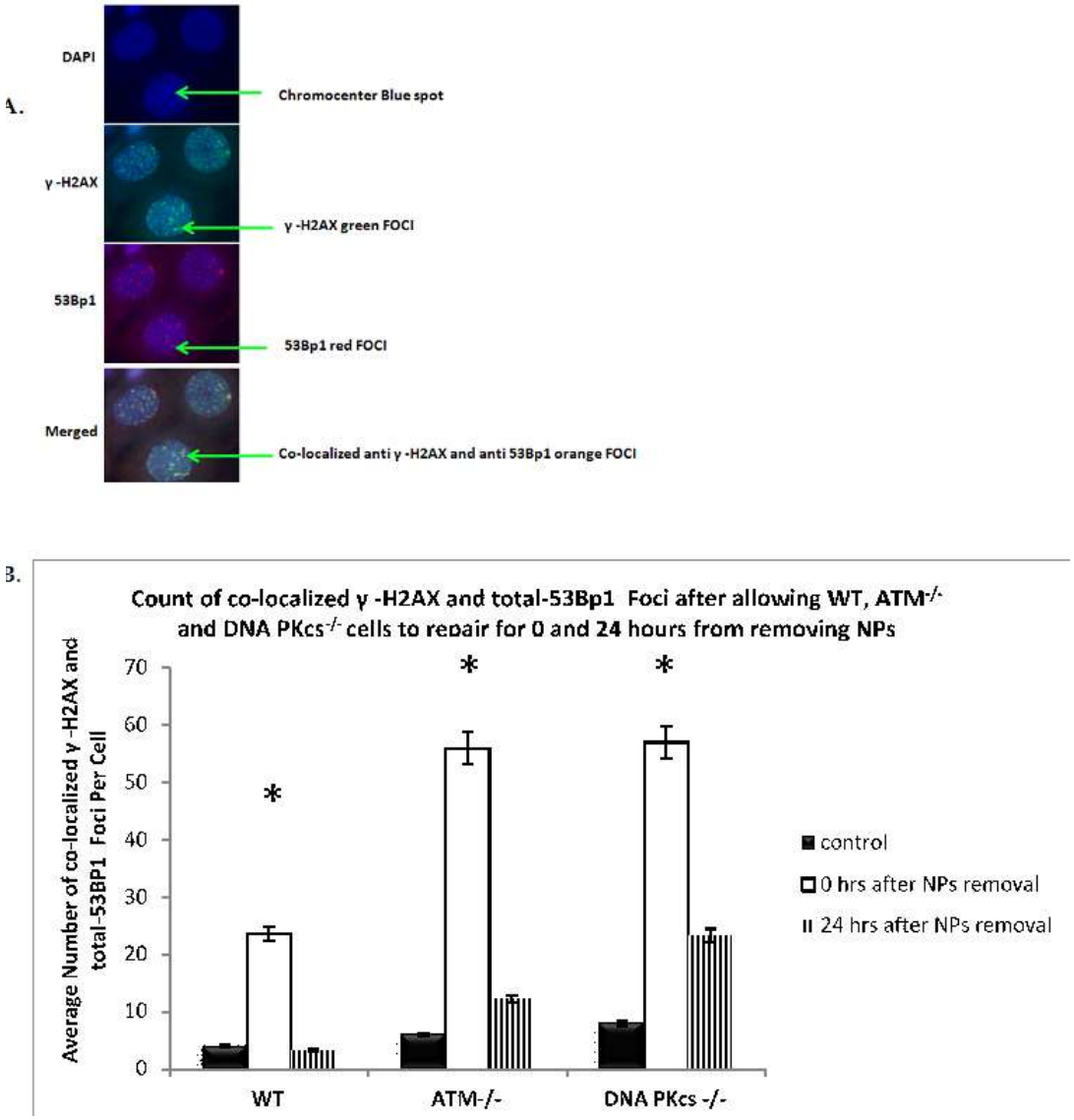

Figure 3. Immunofluorescent visualization of γH2AX and 53BP1, and quantification of DNA double-strand breaks in mouse embryonic fibroblasts, MEFs. (a) Representative 2-D images of WT MEFs nuclei were stained with DAPI (blue nuclei), and cells were stained for phosphorylated H2AX (γH2AX) (green foci) and total-53BP1 (red Foci). TiO_2 NPs induce DSBs that form γH2AX and 53BP1 distinct foci that co-localized in the DAPI stained nuclei showing orange coloration. (b). Bar chart shows the mean number of the co-localized γ-H2AX and total-53BP1 foci per each cell after removing the nanoparticles allowing cells to repair for 0 and 24 hours in WT, $ATM^{-/-}$, and DNA $PKcs^{-/-}$cell lines. A significant increase in the number of co-localized γH2AX and total 53BP1 foci between control and treated cells at 0 hours was observed in the three cell lines ($p<0.05$). After 24 hours from removal of nanoparticles, three cell lines showed a significant decrease in mean number of co-localized γ-H2AX and total-53BP1 foci per cell ($P<0.05$). represented data are mean values from three independent studies.

This was followed by immunofluorescent staining for visualization of DNA double-strand breaks using anti-γ-H2AX and anti-total-53BP1. γ-H2AX foci were found at "chromocenters", the pericentric and centromeric heterochromatin, and the euchromatin regions (Fig. 4). To determine the efficiency of repairing DNA damage at both heterochromatin and euchromatin regions three cell lines WT, $ATM^{-/-}$ and DNA $PKcs^{-/-}$ were allowed to repair for 24 hours after removal of nanoparticles. Then immunofluorescent staining was

performed for the identification of DNA double-strand breaks using anti-γ-H2AX and anti-total-53BP1. As a result, the three cell lines showed a significant decline in the number of DNA breaks after 24 hours of removal of the nanoparticles (Fig. 3b). DNA repair for most of DNA DSBs was observed in WT cells, most of the DNA DSBs at the euchromatin were repaired in ATM$^{-/-}$ cells but DSBs that were near or at chromocenters in ATM$^{-/-}$ cells were left unrepaired. On the other hand, DNA PKcs$^{-/-}$DNA DSBs near the chromocenters were repaired but the DNA DSBs at the euchromatin regions were left unrepaired. Based on these results, we concluded that in G1 phase DNA DSBs repair at the heterochromatin region is ATM-dependent while DNA DSBs repair at the euchromatin region is DNA PKcs dependent (Fig. 4).

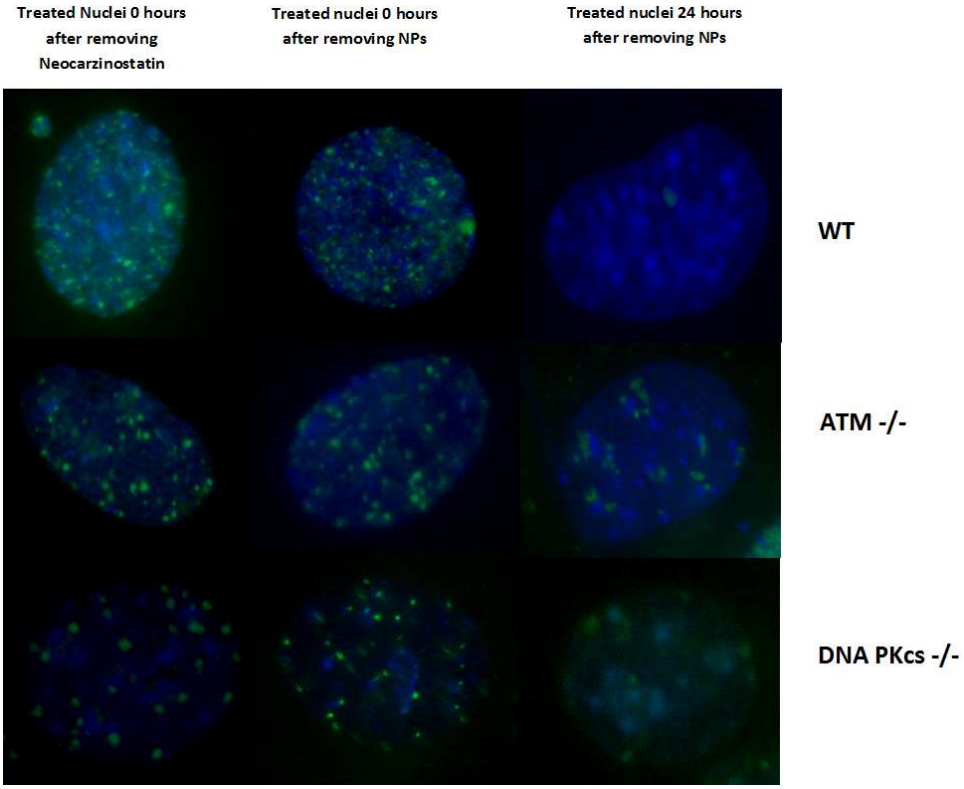

Figure 4. Immunofluorescent visualization of DNA double-strand breaks in WT, ATM$^{-/-}$, and DNA PKC$^{-/-}$cell lines. Representative 2-D images showing that DNA damage persists after 24 hours of exposure to neocarzinostatin (first column), NCS, which is known to be DSBs, is similar to DNA damage persists after 24 hours of exposure to TiO_2 NPs (third column) indicating that the type of DNA damage induced by TiO_2 NPs is DSBs. WT cells showed a lower number of foci than ATM$^{-/-}$ and DNA PKcs$^{-/-}$ after 24 hours of exposure to neocarzinostatin or titanium dioxide NPs reflecting the role of ATM and DNA PKcs in repairing DNA Damage induced by NCS or TiO_2 NPs. Also, the images showed that the DNA damage remained after 24 hours of repair (green spots) in ATM$^{-/-}$ cells were localized near or at the chromocenters of the genome (blue spots). While DNA damage remained after 24 hours repair (green spots) in DNA Pkc $^{-/-}$ cells were localized away from chromocenters (blue spots) and more at the Euchromatin regions of the genome (peripheral sides of the nuclei).

3.3. G2/M checkpoint assay

In order to deeply understand the activation of cell cycle checkpoint which prevents normal, cancer and DNA repair-deficient cells from undergoing mitosis with accumulated DNA damage, a G2/M checkpoint assay was carried out to analyze the efficiency of each cell type in controlling the cell cycle after exposure to the nanoparticles. Thus, we exposed U2OS, A549, and 1Br hTERT cells to different concentrations (0, 0.1, 0.5, 100, 200 μg/ml) for 24 hours. Then immunofluorescent staining for phospho-histone H3 was performed.

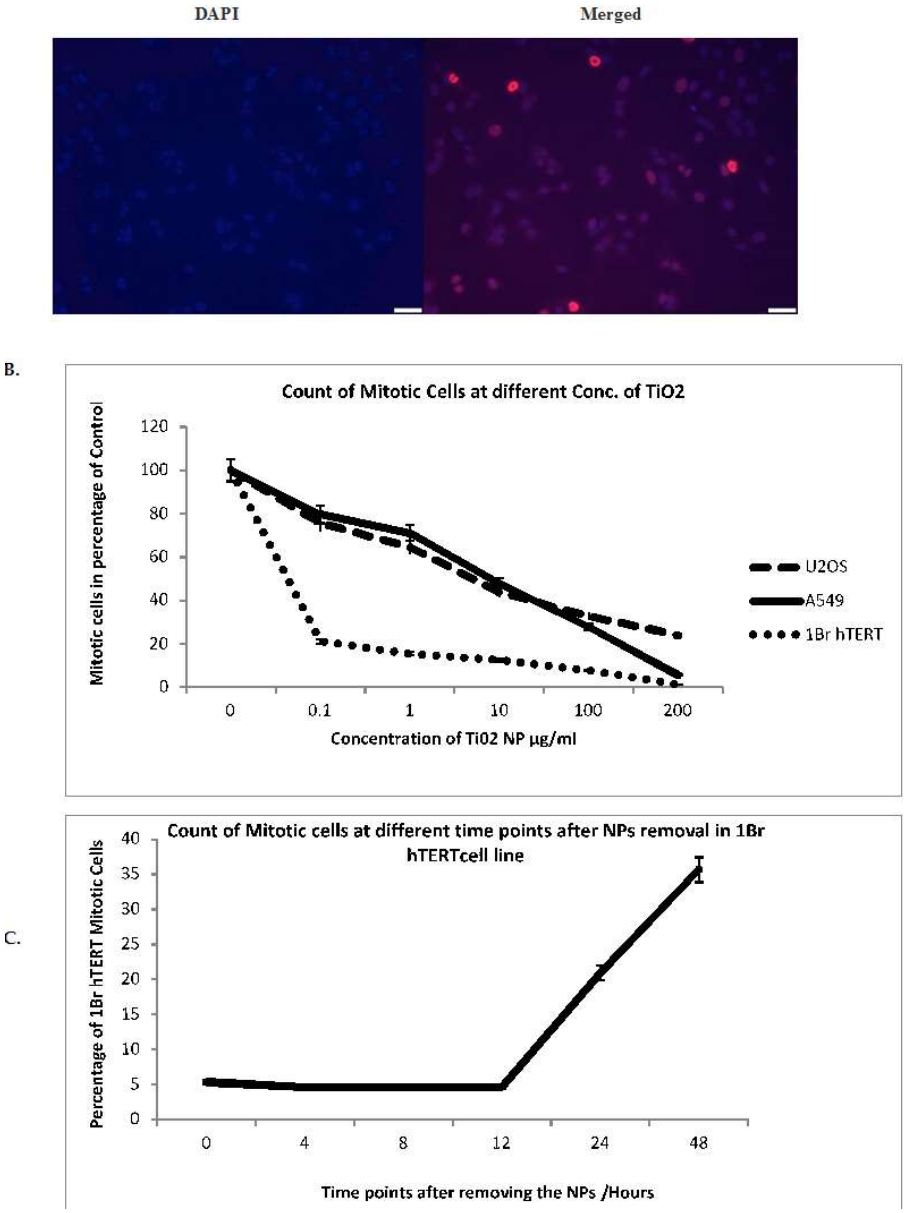

Figure 5. Visualization of mitotic cells by immunofluorescent staining in 1 Br hTERT, U2OS and A549 cell lines that were exposed to different concentrations of nanoparticles for 24 hours. (a) images show staining of nuclei with DAPI (blue) and the staining of phospho-histone H3 in mitotic cells (red). (b) graph shows significant negative relationship between the concentration of TiO_2 nanoparticles and the percentage of mitotic cells in percentage of control in 100 cells of each cell line (1 Br hTERT, U2OS and A549). Quantification of mitotic fraction was performed by counting the mean number of phospho-H3 positive cells per 100 total cells in 1 Br hTERT, U2OS and A549 cell lines that were treated with different concentrations TiO_2 nanoparticles (0, 0.1, 1, 10, 100, 200 µg/ml) for 24 hours. Significant cell cycle arrest with the lowest concentration at $P<0.05$ in 1Br hTERT was observed while no significant arrest at the lowest concentration at $P<0.05$ was observed in U2OS and A549.(c) graph representing the percentage of 1 Br hTERT mitotic cells that was calculated after quantifying the number of phospho-H3 positive cells per 100 cells at different time points (0-4-8-12-24-48 hours) after removal of nanoparticles. cells were treated for 24 hours with the lowest concentration of the nanoparticles (0.1µg/ml) followed by removal of nanoparticles then percentage of mitotic cells was calculated at different time points. significant cell cycle arrest for 12 hours in 1 Br hTERT cells was observed after 12 hours from removal of the nanoparticles. However, after 24 and 48 hours there was significant increase in the percentage of mitotic cells at $P<0.05$. The data was represented after calculating the mean values from three independent experiments.

A.

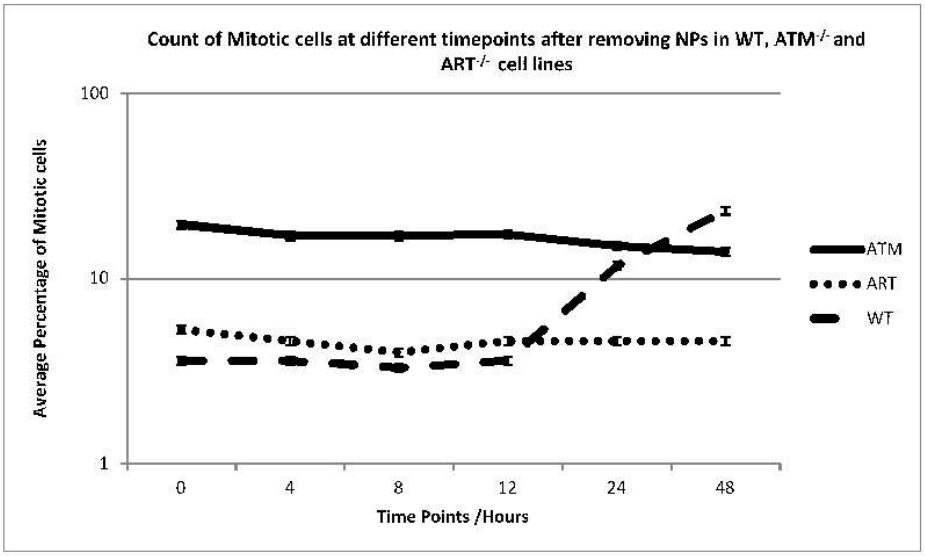

B.

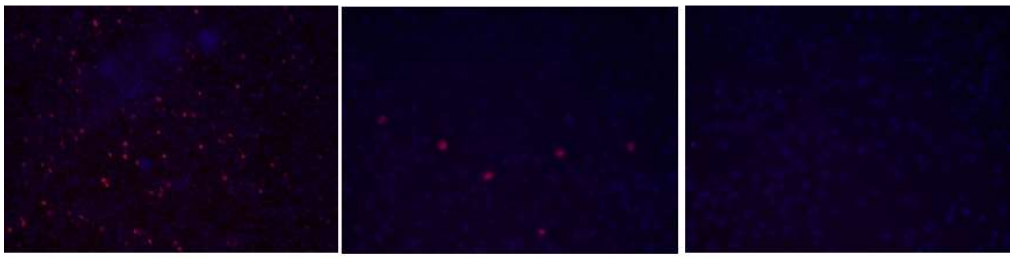

Figure 6. Immunofluorescent detection of Mitotic cells in WT, ATM$^{-/-}$, and ART$^{-/-}$ cell lines that were fixed at different time points after removal of NPs. (a) Representative graph showing the percentage of mitotic cells at different time points after removing the NPs (0, 4, 8, 12, 24, 48 hours). The cells were exposed to the lowest concentration of NPs (0.1 μg/ml) for 24 hours then the NPs were removed and the percentage of Mitotic cells was calculated at different time points (0, 4, 8, 12, 24, 48 hours). ATM$^{-/-}$ cell line showed activated cell cycle while WT and ART$^{-/-}$ cell lines showed an arrested cell cycle for 12 hours. Although ART$^{-/-}$ remained arrested up to 48 hours, WT showed significant increase in the percentage of mitotic cells at 24 and 48 hours ($P<0.05$). (b) 2-D images show presence of mitotic cells for ATM$^{-/-}$ and WT cell lines at 12 hours after removing the NPs while the complete arrest was observed in ART$^{-/-}$ cell line at 12 hours after removing the NPs.

Significant arrest in 1BrhTERT at the lowest concentration of the nanoparticles was observed but significant arrest in U2OS and A549 was observed only after exposure to a high concentration of the nanoparticles (Fig. 5b). In order to know how long will 1Br hTERT cells maintain the cell cycle checkpoint activation, we exposed 1 Br hTERT cells to 0.1 μg/ml TiO_2 nanoparticles for 24 hours this was followed by cell fixation and staining at different time points (0, 4, 8, 12, 24, 48 hours) from nanoparticles removal. Consequently, it was observed that 1 BrHtert cells were able to maintain arrest for only 12 hours after nanoparticles removal (Fig. 5c). Also, WT, ATM$^{-/-}$, ART $^{-/-}$ cells were exposed to 0.1μg/ml TiO_2 nanoparticles for 24 hours then cell fixation and staining performed at different time points after nanoparticles removal (0, 4, 8, 12, 24, 48 hours). ATM$^{-/-}$cells showed no cell cycle arrest but WT and ART $^{-/-}$ showed significant cell cycle arrest. WT cells were able to maintain cell cycle arrest for 12 hours as most DNA breaks were repaired but ART $^{-/-}$ cells kept arrested for 48 hours. This is because ART $^{-/-}$ were not able to repair most of the DNA damage to

be released from cell cycle checkpoint activation (Fig. 6a). The quantification of phospho-histone H3 positive cells was performed per 100 cells in each cell line.

4. DISCUSSION

In this study, we examined the impact of short- and long-term exposures to TiO_2 NPs on U2OS, A549 and 1Br hTERT cell lines. We report that TiO_2 NPs induce significant cytotoxicity at high concentrations (200 μg/ml) over acute exposures, unlike prolonged exposures that showed insignificant cytotoxicity (Fig. 1). However, we did observe significant genotoxicity in both the short- prolonged exposures to TiO_2 NPs. According to the cytotoxic data, it was suggested that the G2/M cell cycle checkpoint was unable in the presence of DNA to maintain cell cycle arrest for a prolonged time. Consequently, in the presence of DNA damage cells were able to divide showing no significant cytotoxicity over prolonged exposures. This was reported before for radiation-induced DSBs [13].

While DNA damage is continually induced during prolonged exposure to TiO_2 NPs, cell cycle arrest is stabilized for long periods of time. However, it was reported that radiation-induced DSBs, lead to cell cycle checkpoint adaptation, making G2/M checkpoint unable to maintain arrest for a long period of time and start mitosis in the presence of DNA damage. Our findings demonstrate that while cells show a significant decline in cell viability after 24 hours of exposure to TiO_2 NPs, it also showed an insignificant decline in cell viability after a 1-week exposure (Figure 1). This indicated that over prolonged exposures, cell cycle arrest was not maintained. Although ongoing DNA repair during the prolonged exposures was possible, we suspected that cells skipped cycle arrest in the presence of DNA damage leading to genetic instability, a hallmark of carcinogenesis.

To test this possibility, we investigated the genotoxic effect of TiO_2 NPs by carrying out immunofluorescent staining for visualization of DNA double-strand breaks after exposing 1 Br hTERT, U2OS and A549 cell lines for different concentrations of TiO_2 NPs (0, 0.1, 0.5, 100, 200 μg/ml) for 24-168 hours. Analysis of γ-H2AX and 53BP1 foci were used as distinct biomarkers for the quantification of DSBs per cell [14]. Using this method, we have shown that short and prolonged exposures induce concentration-dependent genotoxicity, as a concentration of TiO_2 NPs increases, significant increases in the number of foci per cell were observed (Fig. 2). This finding is potentially relevant for human exposure, which takes place in the form of chronic exposure to low concentrations.

Next, the molecular mechanisms enrolled in the activation of the G2/M checkpoint and maintaining cell cycle arrest were studied using WT, ATM-/- and ART-/- cells. We demonstrated that $ATM^{-/-}$ cells were unable at any time point to activate cell cycle checkpoint and arrest mitosis. But $ART^{-/-}$ and WT cells succeeded in activating the cell cycle checkpoint and arresting the cell (Fig. 6a). Thus, we were able to report that ATM is essential for activation of the cell cycle checkpoint to arrest the cell to be able to repair DNA damage caused by TiO_2 NPs. Later after 24 hours from removing the nanoparticles, WT cells were released from checkpoint activation. However, $ART^{-/-}$cells were kept arrested for 48 hours (Fig. 6a). This shows that the cell has a threshold of DNA damage that should fall below it in order to be released from checkpoint activation. This is because WT cells were able to repair most of DNA damage because it has normal DNA repair genes while $ART^{-/-}$ are Artemis deficient cells so they were unable to repair the DNA damage and kept arrested for a longer period of time.

It was previously reported that DNA DSBs induced by ionizing radiation are repaired by fast or slow kinetics depending on the position of DNA double-strand breaks [15]. ATM signaling pathway is activated if DSBs are near or at heterochromatin regions. This is because ATM is needed for heterochromatin relaxation to

facilitate DNA repair (slow kinetics) [15]. On the other hand, ATM and chromatin relaxation are not needed if the damage was at the euchromatin region DNA repair takes place only through c-NHEJ (fast kinetics) [16]. Consequently, we decided to investigate the repair pathways that the cells will use to repair DNA damage induced by TiO_2 NPs through investigating the location of DNA lesions induced by the nanoparticles in G1 synchronized cells. After synchronizing cells WT, $ATM^{-/-}$, and DNA $PKcs^{-/-}$ in the G1 phase, we analyzed which repair kinetics and pathway will repair the DNA lesions, by visualizing the position and counting the number of γ-H2AX foci. The three cell lines were exposed to 0.1 μg/ml TiO_2 NPs for 24 hours. This was followed by immunofluorescent staining for identification of DNA double-strand breaks using antiγ-H2AX and anti 53BP1. As expected, the three cell lines had γ -H2AX foci at heterochromatic as well as euchromatic regions (Fig. 4).

In order to analyze the efficiency of each cell line to repair DNA damage at heterochromatin and euchromatin regions, the three cell lines were allowed to repair for 24 hours after removal of NPs. Most DNA DSBs in WT cells were repaired, while DNA DSBs that were near or at the chromocenters in $ATM^{-/-}$ were left unrepaired (Fig. 4). This was previously shown but for radiation-induced DSBs where ATM signaling is required to promote chromatin relaxation for DNA DSBs repair [15]. Thus, in the absence of ATM, DNA DSBs at heterochromatin caused by the NPs could not also be repaired because DNA repair at heterochromatin region is ATM-dependent. DNA $PKcs^{-/-}$ cells showed a greater repair defect with γ-H2AX foci remaining in both euchromatin and heterochromatin. This was as previously reported for radiation-induced DSBs and consistent with the role of DNA-PKcs in c-NHEJ.

To sum up, we have shown that exposure to TiO_2 NPs induces DNA DSBs that lead to cell cycle checkpoint arrest in an ATM-dependent manner. The repair of these DSBs requires ATM and Artemis when located at heterochromatic regions of the genome whereas a greater fraction of induced DSBs requires DNA-PKcs for efficient repair. These findings show that TiO_2 NPs induced DSBs are repaired by the same mechanisms as ionizing radiation-induced DSBs. Significantly, we have demonstrated that cell cycle checkpoint arrest following prolonged exposure to TiO_2 NPs induced DNA DSBs is not maintained, leading to cells entering mitosis in the presence of DNA damage.

5. CONCLUSION

Prolonged exposure to low concentrations of TiO_2 NPs induces significant genotoxicity and insignificant cytotoxicity. This is because cells were unable to maintain cell cycle arrest for a long period of time due to cell cycle checkpoint adaptation. Consequently, cells are released from the cell cycle checkpoint only after the amount of DNA damage falls below a certain threshold entering mitosis with remaining DNA damage leading to genetic instability. Furthermore, we demonstrated in this study that ATM is needed for activation of cell cycle checkpoint for DNA repair following TiO_2 NPs induced DNA damage. Lastly, DNA repair for DSB induced by TiO_2 NPs near heterochromatin region is ATM-dependent while DSB induced by TiO_2 NPs near euchromatin is DNA Pkcs dependent.

Authors' contributions: AK designed the study and supervised the project. NE carried out the experiments and wrote the manuscript with support from AK. Both authors discussed the results and contributed to the final manuscript.

Conflict of interest: The authors declare no potential conflict of interest.

REFERENCES

1. Skocaj M, Filipic M, Petkovic J, Novak S. Titanium dioxide in our everyday life; is it safe? Radiol Oncol. 2011; 45(4): 227–247.

2. Rollerova E, Tulinska J, Liskova A, Kuricova M, Kovriznych J, Mlynarcikova A, et al. Titanium dioxide nanoparticles: some aspects of toxicity/focus on the development. Endocr Regul. 2015; 49(02): 97–112.
3. Zhang XZ, Sun HW, Zhang ZY. [Bioaccumulation of titanium dioxide nanoparticles in carp]. Huan Jing Ke Xue Huanjing Kexue Bian Ji Zhongguo Ke Xue Yuan Huan Jing Ke Xue Wei Yuan Hui Huan Jing Ke Xue Bian Ji Wei Yuan Hui. 2006; 27(8): 1631–1635.
4. Johnston HJ, Hutchison GR, Christensen FM, Peters S, Hankin S, Stone V. Identification of the mechanisms that drive the toxicity of TiO2 particulates: the contribution of physicochemical characteristics. Part Fibre Toxicol. 2009; 6(1): 33.
5. Park EJ, Yi J, Chung KH, Ryu DY, Choi J, Park K. Oxidative stress and apoptosis induced by titanium dioxide nanoparticles in cultured BEAS-2B cells. Toxicol Lett. 2008; 180(3): 222–229.
6. Gurr JR, Wang ASS, Chen CH, Jan KY. Ultrafine titanium dioxide particles in the absence of photoactivation can induce oxidative damage to human bronchial epithelial cells. Toxicology. 2005; 213(1–2): 66–73.
7. Zhu Y, Eaton JW, Li C. Titanium Dioxide (TiO_2) Nanoparticles Preferentially Induce Cell Death in Transformed Cells in a Bak/Bax-Independent Fashion. Plos One. 2012; 7(11): e50607.
8. Schilling K, Bradford B, Castelli D, Dufour E, Nash JF, Pape W, et al. Human safety review of "nano" titanium dioxide and zinc oxide. Photochem Photobio S. 2010; 9(4): 495–509.
9. Chen X, Selloni A. Introduction: Titanium Dioxide (TiO2) Nanomaterials. Chem Rev. 2014; 114(19): 9281–9282.
10. Jugan ML, Barillet S, Simon-Deckers A, Herlin-Boime N, Sauvaigo S, Douki T, et al. Titanium dioxide nanoparticles exhibit genotoxicity and impair DNA repair activity in A549 cells. Nanotoxicology. 2011; 6(5): 501–513.
11. Weir A, Westerhoff P, Fabricius L, Hristovski K, Goetz N von. Titanium Dioxide Nanoparticles in Food and Personal Care Products. Environ Sci Technol. 2012; 46(4): 2242–2250.
12. Riballo E, Kühne M, Rief N, Doherty A, Smith GCM, Recio MJ, et al. A Pathway of Double-Strand Break Rejoining Dependent upon ATM, Artemis, and Proteins Locating to γ-H2AX Foci. Mol Cell. 2004; 16(5): 715–724.
13. Löbrich M, Jeggo PA. The impact of a negligent G2/M checkpoint on genomic instability and cancer induction. Nat Rev Cancer. 2007; 7(11): 861–869.
14. Stope M. Phosphorylation of histone H2A.X as a DNA-associated biomarker (Review). World Acad Sci J. 2021; 3: 3.
15. Goodarzi AA, Noon AT, Deckbar D, Ziv Y, Shiloh Y, Löbrich M, et al. ATM Signaling Facilitates Repair of DNA Double-Strand Breaks Associated with Heterochromatin. Mol Cell. 2008; 31(2): 167–177.
16. Iliakis G, Murmann T, Soni A. Alternative end-joining repair pathways are the ultimate backup for abrogated classical non-homologous end-joining and homologous recombination repair: Implications for the formation of chromosome translocations. Mutat Res Genetic Toxicol Environ Mutagen. 2015; 793: 166–175.